INFECTION AND IMMUNITY, Oct. 1997, p. 4243–4249 Vol. 65, No. 10
0019-9567/97/$04.00+0

Involvement of p21^{racA}, Phosphoinositide 3-Kinase, and Vacuolar ATPase in Phagocytosis of Bacteria and Erythrocytes by *Entamoeba histolytica*: Suggestive Evidence for Coincidental Evolution of Amebic Invasiveness

SUDIP K. GHOSH AND JOHN SAMUELSON*

Department of Tropical Public Health, Harvard School of Public Health, Boston, Massachusetts 02115

Received 22 May 1997/Returned for modification 20 June 1997/Accepted 17 July 1997

Trophozoites of *Entamoeba histolytica*, the protozoan parasite that causes amebic dysentery, phagocytose bacteria in the colonic lumen and erythrocytes (RBC) in host tissues. Because tissue invasion is an evolutionary dead end, it is likely that amebic pathogenicity is coincidentally selected, i.e., the same methods used to kill bacteria in the colonic lumen are used by parasites to damage host cells and cause disease. In support of this idea, the amebic lectin and pore-forming peptide are involved in binding and killing, respectively, bacteria and host epithelial cells. Here amebic phagocytosis of bacteria, RBC, and mucin-coated beads was disrupted by overexpression of *E. histolytica* p21$^{racA\text{-}V12}$, a *ras*-family protein involved in selection of sites of actin polymerization, which had been mutated to eliminate its GTPase activity. p21$^{racA\text{-}V12}$ transformants were also defective in capping and cytokinesis, while pinocytosis of fluorescent dextrans was not affected. Wortmannin, a fungal inhibitor of phosphoinositide 3-kinase, markedly inhibited phagocytosis of bacteria, RBC, and mucin-coated beads by wild-type amebae. In contrast to p21$^{racA\text{-}V12}$ overexpression, wortmannin abolished amebic pinocytosis of dextrans but had no inhibitory effects on capping. Inhibition of amebic vacuolar acidification by bafilomycin also decreased bacterial and RBC uptake. These results, which demonstrate similarities between mechanisms of phagocytosis of bacteria and RBC by amebae and macrophages, support the idea of coincidental selection of amebic genes encoding proteins that mediate destruction of host cells.

Entamoeba histolytica is an amitochondriate protozoan parasite, which causes dysentery and liver abscess in developing countries, where its fecal-oral spread cannot be prevented (34, 40). *Entamoeba dispar* is a closely related enteric protozoan parasite, which does not cause dysentery or liver abscess (15). Trophozoites (ameboid forms) of *E. histolytica* and *E. dispar* grow under anaerobic conditions in the lumen of the distal colon, where they consume bacteria as their nutrient source (36, 44). In the colonic lumen, trophozoites transform to cysts, which have four nuclei and a chitin wall. Cysts are the infectious stage of the parasite, because they are resistant to attack by stomach acids, duodenal proteases, and bile (40). Tissue invasion by *E. histolytica* is an evolutionary dead end because trophozoites do not form cysts in tissues, patients with amebic dysentery shed fewer infectious cysts and more noninfectious trophozoites, and liver abscesses are potentially fatal to the host (6, 8, 34).

In the absence of selection, it is not obvious how *E. histolytica* genes involved in tissue invasion are retained. Here we suggest that these genes, which encode amebic proteins that damage host cells, are maintained by coincidental selection, i.e., these same proteins are involved in phagocytosis of bacteria within the colonic lumen, where amebae do not cause disease (19, 29, 35, 43). In support of the idea of coincidental selection, phagocytosis-deficient parasites selected with bromodeoxyuridine-labeled bacteria are less pathogenic than wild-type parasites (46), addition of bacteria to axenic parasites causes them to be more virulent (36), lectins mediate amebic phagocytosis of bacteria and epithelial cells (32, 36, 42), and amebae make pore-forming peptides (PFP; also known as amebapores), which are lytic to bacteria and epithelial cells (27, 28). Similarly, NK lysins, which are mammalian homologs of amebic PFP, are lymphocyte proteins involved in bacterial killing and tumor cell lysis (3). Other infectious examples of coincidental selection include *Escherichia coli* urinary tract infections, which are mediated by pili that also attach bacteria to gastrointestinal epithelial cells, and cerebral malaria, which involves knob proteins that also sequester parasites away from the spleen (29, 33).

A prediction of the idea of coincidental selection amebic tissue invasion is that proteins involved in host cell lysis will also be involved in bacterial killing. In the case of the amebic lectin and PFP, these experiments have already been performed (27, 28, 32, 42). Our goal was to study a number of other amebic proteins which may be involved in host cell and bacterial killing. Three amebic proteins (p21^{rac}, phosphoinositide 3-kinase [PI 3-kinase], and vacuolar proton-transporting ATPase [V-ATPase]) were tested because they are involved in killing of bacteria and senescent erythrocytes (RBC) by macrophages (4, 12, 18, 22, 31, 37). p21^{rac} proteins, members of the *ras* family of signal-transducing proteins, are low-molecular-weight GTP-binding proteins, important for site selection of actin polymerization (1, 22, 38, 45). Amebae have at least seven different *rac* genes, one of which encodes p21^{racA}, which shows >70% positional identities with p21^{rac1} of *Dictyostelium discoideum*, humans, *Drosophila melanogaster*, and *Caenorhabditis elegans* (10, 11, 21, 31, 49).

PI 3-kinases are a family of enzymes with 100-kDa catalytic subunits and an 85-kDa regulatory subunit, which has SH2, SH3, and BCR domains (50). PI 3-kinases, which phosphorylate phosphoinositides, are involved in signal transduction in

* Corresponding author. Mailing address: Department of Tropical Public Health, Harvard School of Public Health, 665 Huntington Ave., Boston, MA 02115. Phone: (617) 432-4670. Fax: (617) 738-4914. E-mail: jsamuels@hsph.harvard.edu.

response to insulin, nerve growth factor, histamine, and some cytokines. PI 3-kinases are irreversibly inhibited by the cell-permeable fungal protein wortmannin, which covalently modifies Lys-802 in the catalytic subunit (54). Wortmannin inhibits macropinocytosis, Fcγ receptor signaling, and phagocytosis by macrophages (4, 37).

Phagolysosomal acidification, which is inhibited by the weak base monensin or ammonium chloride, is necessary for contact-mediated cytolysis of host epithelial cells by amebae (41, 48). Bafilomycin A, a specific inhibitor of V-ATPases, inhibits acidification of pinocytotic vacuoles (7, 30). Amebic genes encoding the catalytic peptide (ATPase) and proteolipid (transmembrane domain) of the V-ATPase have been cloned previously (14, 47, 55). Vacuolar acidification is also essential for bacterial killing by macrophages (18).

Here cultured amebae were transformed with an *E. histolytica racA* gene encoding a p21^{racA} protein with a Gly-12-Val mutation, which eliminates its GTPase activity and causes this regulatory protein to remain constantly in the active state. The ability of p21$^{racA\text{-}V12}$-transfected amebae to phagocytose bacteria, RBC, and mucin-coated beads was determined (17). Transformed amebae were also incubated with fluorescein isothiocyanate (FITC)-conjugated dextran and FITC-concanavalin A (ConA) to determine the effect of p21$^{racA\text{-}V12}$ overexpression on pinocytosis and capping, respectively (16, 30). The effects of wortmannin, bafilomycin, monensin, and ammonium chloride on phagocytosis of bacteria and RBC by wild-type amebae were also determined.

The last proteins tested were amebic cysteine proteases (encoded by at least five genes), which have been implicated in epithelial cell destruction, degradation of the extracellular matrix, and abscess formation (9, 24, 39, 51). The cysteine protease inhibitor E-64, at concentrations that inhibited abscess formation, as well as three other cysteine protease inhibitors, was assayed for its ability to inhibit amebic phagocytosis of bacteria and RBC.

MATERIALS AND METHODS

Construction of the pJST4-RacA-V12 vector and transformation of *E. histolytica*. The *E. histolytica racA* gene was modified in two ways before cloning into the pJST4 vector using synthetic oligonucleotides and PCR (Fig. 1) (17). First, 27 bp encoding the hemagglutinin antigen (HA) of influenza virus (YPYDVPDYA) was added to the 5′ end of the *racA* gene (the amino terminus of p21^{racA}) (53). Second, *E. histolytica* p21^{racA} was aligned with human p21^{rac1} to identify the Gly residue, which, when mutated to Val, disrupts the GTPase activity of the proteins and so fixes p21^{rac} in the active state (22). The *E. histolytica racA* gene was mutagenized to encode p21^{racA} with a Gly-12-to-Val-12 mutation. The twice-modified *E. histolytica racA* gene was cloned into pJST4 to make the pJST4-RacA-V12 vector, which was sequenced to confirm the presence of the intended modifications. The pJST4-RacA-V12 vector was electroporated into *E. histolytica* HM-1 amebae and selected with G418 to a final concentration of 50 μg/ml (22).

Expression of p21$^{racA\text{-}V12}$ by transformed parasites was confirmed in two ways. First, total RNA of transformed and nontransformed parasites (control) was purified with an RNA Easy kit (Qiagen) and treated with RNase-free DNase (Pharmacia) to remove contaminating DNA. Reverse transcriptase PCR (RT-PCR) was performed with primers to the HA epitope and to the 3′ end of the *racA* gene. Positive controls included primers to amebic actin genes, while negative controls omitted RT. Second, total proteins of amebae were lysed in sodium dodecyl sulfate and β-mercaptoethanol, electrophoresed on sodium dodecyl sulfate-polyacrylamide gel electrophoresis gels containing 15% acrylamide, and transferred to polyvinylidene difluoride membranes. Membranes were incubated with a mouse monoclonal antibody against the HA epitope (Boehringer), and bound mouse antibodies were detected with a chemiluminescence kit (Amersham) (53).

Light and scanning electron microscopy of cultured parasites. Nontransformed amebae and p21$^{racA\text{-}V12}$ transformants were observed in 50-ml flasks with an inverted-phase microscope to determine whether there were dysmorphic amebae among the latter. Differences in the rate of cytokinesis were estimated by measuring the time it took for 20 nontransformed amebae and 20 p21$^{racA\text{-}V12}$ transformants to complete binary fission.

To visualize filamentous actin within nontransformed amebae and p21$^{racA\text{-}V12}$ transformants, parasites were fixed for 10 min by addition of 2% paraformaldehyde to the medium at 37°C, permeabilized by incubation in 0.1% Triton X-100 for 10 min, and then washed and incubated with 0.1-mg/ml phalloidin, which was labeled with FITC (Sigma) for 1 h (5, 13, 20). Unbound FITC-phalloidin was washed with phosphate-buffered saline (PBS), and the trophozoites were examined under the Leitz Orthoplan fluorescence microscope.

For scanning microscopy, parasites were fixed briefly at 37 and then at 4°C for 1 h in 1% glutaraldehyde–3% formaldehyde in phosphate buffer, postfixed at 4°C for 1 h in 1% osmium tetroxide, dehydrated in graded ethanols, critical point dried, and coated with gold-palladium. Parasites were observed with a Amray 100A scanning electron microscope with an LaB_6 filament.

Capping, pinocytosis, and phagocytosis assays. Capping was induced by incubating trophozoites for 30 min at 4°C with 20-μg/ml FITC-ConA in PBS (2, 16). Parasites were washed at 4°C, incubated at 37°C for 10 min, fixed in 2% paraformaldehyde, and examined under the fluorescence microscope.

Pinocytosis was observed by incubating trophozoites for 10 or 30 min at 37°C with FITC-dextran (1 mg/ml) in complete TYI-SS medium (30, 47). Amebae were washed in PBS, fixed in 2% paraformaldehyde, and passed through a Callibar (Becton Dickinson) fluorescence-activated cell sorter (FACS). Negative controls included paraformaldehyde-fixed parasites not exposed to FITC-dextran.

Phagocytosis by amebae was studied with fluorescent beads, human RBC (type O^+), and bacteria expressing recombinant green fluorescent protein (GFP) under an isopropyl-β-D-thiogalactopyranoside (IPTG)-inducible promoter (52). Four types of fluorescent beads were tested for their ability to be phagocytosed by amebae: uncoated beads, beads covered with bovine serum albumin to give them a negative charge, beads covered with aliphatic amine to give them a positive charge, and beads covered with colonic mucin (25). Trophozoites (10^5/ml) were incubated in TYI-SS medium at 37°C with beads (10^7/ml), RBC (10^7/ml), or IPTG-induced bacteria (10^7/ml) for 10 or 30 min and then fixed with 2% paraformaldehyde in PBS. Phagocytosed beads and bacteria were counted with the fluorescence microscope, with some bright-field illumination to identify the edges of the cells. Phagocytosed RBC were counted in bright field. Lysis of RBC and bacteria was judged when hemoglobin pigment or GFP, respectively, diffusely filled phagocytotic vacuoles. All experiments were repeated at least three times.

Treatment of wild-type parasites with wortmannin, ammonium chloride, monensin, and E-64. To test the effect of PI 3-kinase inhibition, amebae were preincubated with 100 nM wortmannin for 1 h at 37°C, and the same concentration of drug was maintained after addition of bacteria, RBC, mucin-coated beads, FITC-dextran, or FITC-ConA (4, 37, 54). To test the effect of inhibition of vacuolar acidification, amebae were preincubated with 100-μg/ml bafilomycin, 2 μM monensin, or 30 mM ammonium chloride, and the same concentration of each drug was maintained after addition of bacteria or RBC (7, 18, 30). To test the effect of inhibition of cysteine proteases, amebae were preincubated with 100 nM E-64, 10-μg/ml *Z*-L-Leu-L-Tyr-CHN_2, 100-μg/ml phenylmethylsulfonyl fluoride, or 5-μg/ml leupeptin, and the same concentration of drug was maintained after addition of bacteria (9, 24, 39).

RESULTS

Morphological comparison of nontransformed amebae and p21$^{racA\text{-}V12}$ transformants. Overexpression of p21$^{racA\text{-}V12}$ by transformed parasites, selected with G418, was confirmed by RT-PCR with primers to the HA epitope and to the 3′ end of the *racA* gene and by Western blotting with an anti-HA epitope monoclonal antibody (Fig. 1). Control RT-PCR and Western blotting were negative with nontransformed parasites. The pJST4-RacA-V12 plasmid was recovered intact from transformed parasites, suggesting that the vector was replicating as an episomal element (data not shown) (17).

Although the growth rate of p21$^{racA\text{-}V12}$ transformants was nearly the same as those of nontransformed amebae, there appeared to be a defect in cell division in the former. Dividing forms were frequent in cultures of p21$^{racA\text{-}V12}$ transformants, while they were rare in nontransformed amebae (Fig. 2). On average, p21$^{racA\text{-}V12}$ transformants took 6 ± 1 min to complete cell division, while nontransformed parasites took 3 ± 1 min to divide. This result suggests that p21^{racA} may contribute to binary fission in this parasite, which is remarkable for the presence of actin in the narrow isthmus between dividing amebae (20).

The p21$^{racA\text{-}V12}$ transformants were motile, and scanning microscopy showed little difference between p21$^{racA\text{-}V12}$ transformants and nontransformed parasites (data not shown). In contrast, hyperactive p21^{rac} causes increased ruffling in mac-

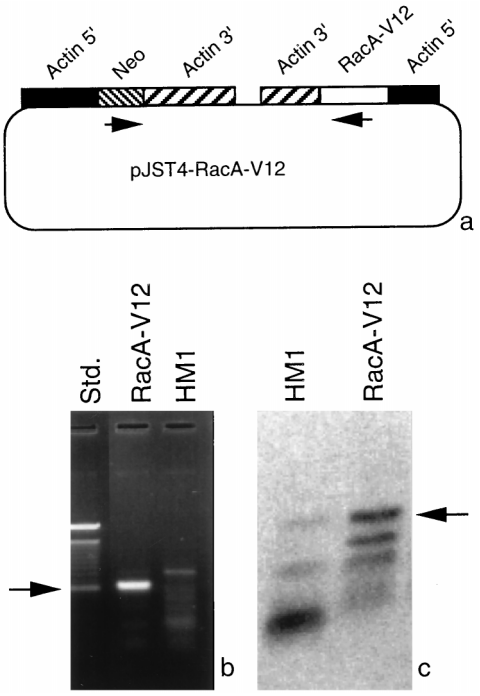

FIG. 1. Expression of p21$^{racA\text{-}V12}$ by transformed parasites. Shown are the pJST4-RACA-V12 vector (a) used to transform parasites and RT-PCR products (b) with a sense primer to the HA epitope and an antisense primer to the 3′ end of the *E. histolytica racA* open reading frame. The 618-bp product (arrow) was present in p21$^{racA\text{-}V12}$ transformants but was absent in nontransformed parasites (HM1). Also shown is a Western blot (c) with a mouse monoclonal antibody to the HA epitope. A 23-kDa band (arrow) was present in p21$^{racA\text{-}V12}$ transformants and was absent in nontransformed parasites. Lower-molecular-weight bands in transformed parasites reacting with the HA antibody likely represent degraded p21$^{racA\text{-}V12}$.

rophages as shown by scanning microscopy (22, 38, 45). Phalloidin staining of filamentous actin demonstrated a second defect in these mutant parasites. Prominent actin stress fibers and cup-like accumulations of actin under the plasma membrane were much more frequent in p21$^{racA\text{-}V12}$ transformants than in nontransformed parasites (Fig. 2). In nontransformed amebae, prominent actin stress fibers are rare, while cup-like accumulations of actin are associated with phagocytosis of RBC (5, 13, 16).

Interactions of p21$^{racA\text{-}V12}$ transformants with their environment. Overexpression of p21$^{racA\text{-}V12}$ had profound effects on rates of phagocytosis of bacteria, RBC, and mucin-coated beads and inhibited amebic capping but had no effect on pinocytosis of dextran or lysis of phagocytosed bacteria and RBC (see Fig. 3 to 7).

Phagocytosis of bacteria. In the colonic lumen, amebae consume bacteria by phagocytosis (36). *E. coli* cells expressing recombinant GFP under an IPTG-inducible promoter were used to study amebic phagocytosis because these bacteria were very bright and easy to see when phagocytosed by amebae (Fig. 3) (51). More than 40% of nontransformed amebae phagocytosed >10 bacteria/ameba within 10 min, while 25% of these amebae phagocytosed <6 bacteria. Heterogeneity in the number of bacteria (as well as RBC and beads [see below]) consumed by nontransformed amebae was likely secondary to the use of unsynchronized parasites in these studies. In contrast, only 9% of p21$^{racA\text{-}V12}$ transformants phagocytosed >10 bacteria, while 52% of p21$^{racA\text{-}V12}$ transformants phagocytosed <6 bacteria. These results suggest that overexpression of p21$^{racA\text{-}V12}$ disrupts amebic phagocytosis of bacteria, as has been shown elsewhere for macrophages (12).

Killing of phagocytosed bacteria, judged by release of GFP into the vacuole, however, appeared similar for nontransformed amebae and p21$^{racA\text{-}V12}$ transformants (Fig. 3). Both groups of parasites started killing bacteria after ~30 min of intake, and killing was nearly complete for both groups after 90 min. These killing times are somewhat shorter than those previously reported for amebae but are not dissimilar to those reported for macrophages elsewhere (4, 20).

Phagocytosis of RBC. p21$^{racA\text{-}V12}$ transformants were also defective in the uptake of human RBC versus nontransformed amebae (Fig. 4). Most of the bound RBC were taken into phagocytotic vacuoles of nontransformed amebae within 10 min at 37°C. In contrast, most of the bound RBC remained on the surface of p21$^{racA\text{-}V12}$ transformants, often in large aggregates. Sixty percent of nontransformed amebae phagocytosed >10 RBC per parasite, while 25% took up <6 RBC. In contrast, 15% of p21$^{racA\text{-}V12}$ transformants phagocytosed >10 RBC, while 65% phagocytosed <6 RBC. Lysis of phagocytosed RBC, detected by spilling of hemoglobin pigment into the vacuole, appeared to be unchanged for p21$^{racA\text{-}V12}$ transformants (data not shown). Lysis of RBC and bacteria by the transformants suggests that fusion of phagosomes with lysosomes was not impaired by overexpression of hyperactive p21^{racA}.

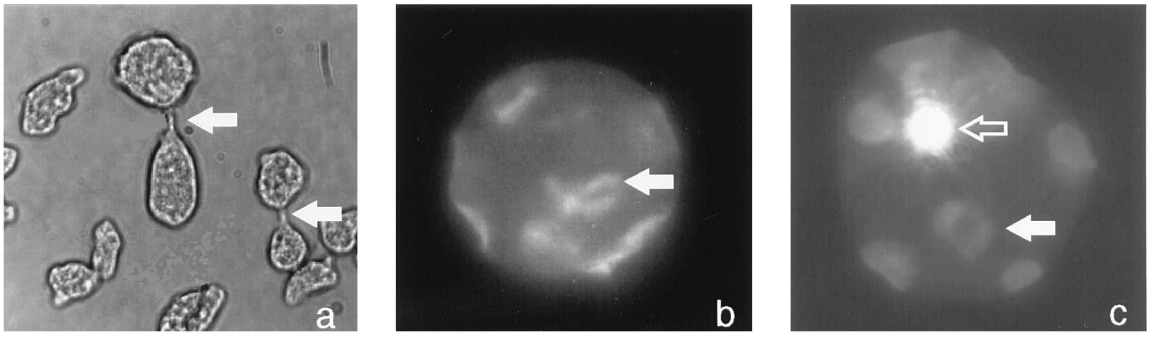

FIG. 2. Photomicrographs of p21$^{racA\text{-}V12}$ transformants in culture. Multiple dividing transformants were present within the same high-powered field (a). Indirect immunofluorescence of phalloidin-stained transformants showed numerous cells with prominent actin stress fibers (arrow in panel b) and cup-shaped accumulations of actin beneath the plasma membrane (solid arrow in panel c). The fluorescent bead (open arrow in panel c) was independent of the cup-shaped accumulations of actin.

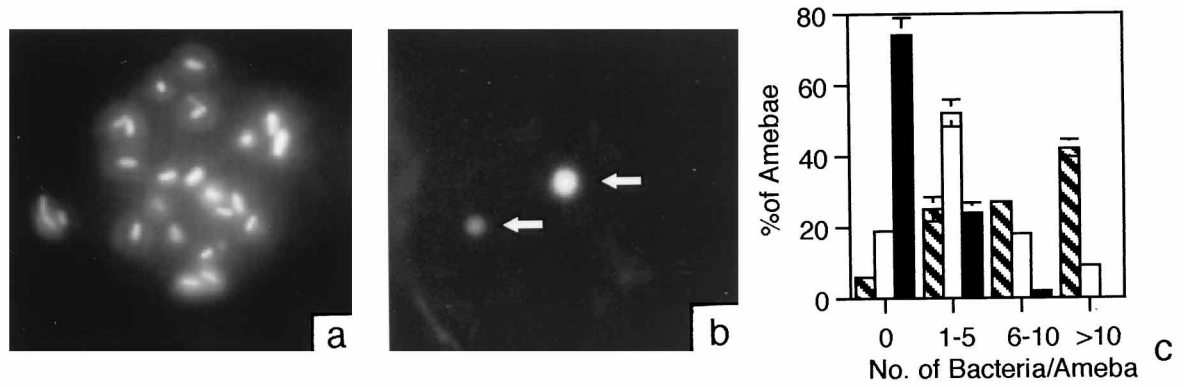

FIG. 3. Phagocytosis of bacteria expressing GFP by nontransformed amebae and p21$^{racA\text{-}V12}$ transformants. Nearly half of nontransformed amebae (a) accumulated >10 bacteria. Lysed bacteria within phagocytotic vacuoles of p21$^{racA\text{-}V12}$ transformants (b) lost their rod-like shape (arrows). Also shown is a bar graph (c) plotting the number of bacteria per cell for nontransformed amebae (striped bars), p21$^{racA\text{-}V12}$ transformants (open bars), and bafilomycin-treated, wild-type amebae (solid bars). Error bars indicate standard deviations of three experiments. Where no error bars are present, standard deviations were too small to be plotted. Uptake of bacteria in the presence of wortmannin was completely inhibited (data not shown).

Phagocytosis of beads. Parasites took up few beads that were uncoated, negatively charged, or positively charged (data not shown). In contrast, amebae rapidly phagocytosed mucin-coated beads, demonstrating that bead uptake is specific and is likely accomplished by means of lectins on the parasite surface (Fig. 5) (32, 42). Mucin beads were very bright and of uniform size, did not quench with prolonged UV exposure, were not degraded by the parasites, and so were easy to count with the fluorescence microscope. Nontransformed parasites consumed 16 ± 9 beads/parasite (average and standard deviation, respectively), with 67% taking up >11 beads. In contrast, p21$^{racA\text{-}V12}$ transformants consumed 10 ± 8 beads/parasite ($P < 0.001$ versus nontransformed amebae), with only 37% taking up >11 beads.

Pinocytosis. Amebae pinocytose as much as 30% of their volume per hour (30). Here nontransformed amebae and p21$^{racA\text{-}V12}$ transformants took up FITC-dextran into small vacuoles (as shown in Fig. 1 of reference 47) at nearly the same rates when measured by FACS (Fig. 6). This result suggests that amebic pinocytosis was not disrupted by overexpression of p21$^{racA\text{-}V12}$.

Capping. Capping of bound antibodies and their release by shedding, which is mediated by actin and myosin II, have been suggested as a mechanism by which amebae avoid the host immune response (2, 16, 20). Ninety-six percent of all nontransformed amebae form a single cap on their surface when incubated with the multivalent ligand FITC-ConA, while 4% had two caps (Fig. 7). In contrast, only 71% of p21$^{racA\text{-}V12}$ transformants formed a single cap, 14% of transformed amebae had two caps per cell, 5% had three caps per cell, and 10% had no caps. Similar capping results were seen when a mutated p21^{racG} was overexpressed (21).

Wortmannin inhibited amebic pinocytosis and phagocytosis of bacteria, RBC, and mucin-coated beads but had no effect on capping. Wortmannin, an inhibitor of PI 3-kinase, completely abolished uptake of bacteria and RBC by amebae (data not shown). Only 38% of wortmannin-treated amebae took up >10 beads, a result similar to that for p21^{racA} transformants (Fig. 5). Wortmannin also completely inhibited pinocytosis of FITC-dextran (Fig. 6). Wortmannin inhibits pinocytosis of high-molecular-weight dextrans and phagocytosis by macrophages (4). Wortmannin had no effect on amebic capping, as 95% of parasites treated with wortmannin formed a single, normal-looking cap with FITC-ConA, while 4% had two caps, and 1% had no cap. These results are different from those for

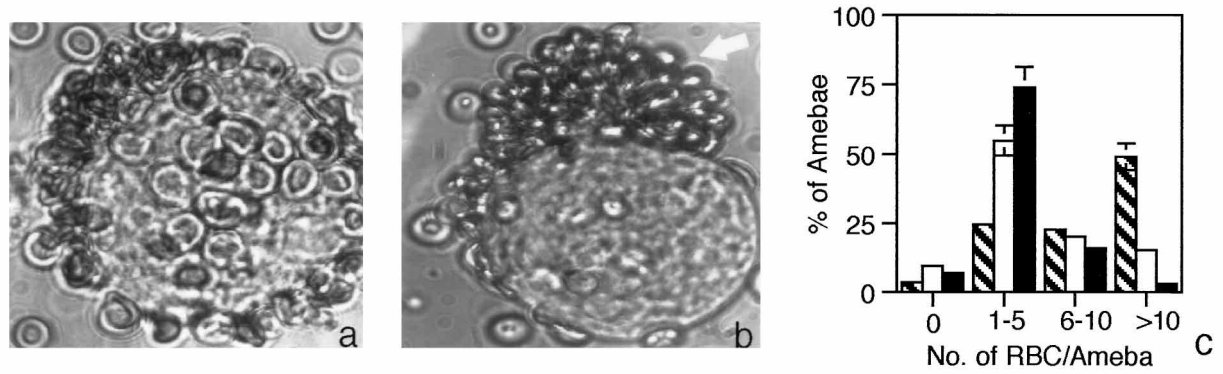

FIG. 4. Phagocytosis of RBC by nontransformed amebae and p21$^{racA\text{-}V12}$ transformants. Most nontransformed amebae (a) phagocytosed >10 RBC, with many more RBC present diffusely on the parasite surface. In contrast, most p21$^{racA\text{-}V12}$ transformants (b) phagocytosed <6 RBC, with many RBC accumulating in a cap-like structure on the parasite surface. Also shown is a bar graph (c) plotting the number of RBC per cell for nontransformed amebae (striped bars), p21$^{racA\text{-}V12}$ transformants (open bars), and bafilomycin-treated, wild-type amebae (solid bars). Error bars indicate standard deviations of three experiments. Uptake of RBC in the presence of wortmannin was completely inhibited (data not shown).

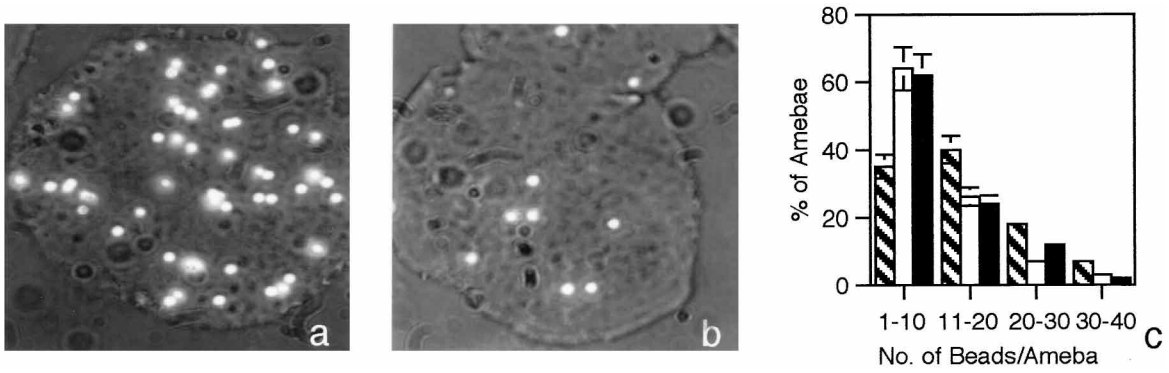

FIG. 5. Phagocytosis of mucin-coated fluorescent beads by nontransformed amebae and p21$^{racA\text{-}V12}$ transformants. Most nontransformed parasites (a) accumulated >10 mucin beads per cell. In contrast, most p21$^{racA\text{-}V12}$ transformants (b) and wild-type amebae treated with wortmannin (not shown) accumulated <11 mucin beads. Also shown is a bar graph plotting the number of mucin beads per parasite for nontransformed amebae (striped bars), p21$^{racA\text{-}V12}$ transformants (open bars), and wortmannin-treated, wild-type parasites (closed bars). Error bars indicate standard deviations of three experiments.

overexpression of p21$^{racA\text{-}V12}$, in which capping was inhibited in many cells while pinocytosis was not affected.

Raising vacuolar pH inhibited phagocytosis of bacteria and RBC. Inhibition of vacuolar acidification partially inhibits amebic pinocytosis and blocks amebic lysis of epithelial cells in vitro (30, 41). Vacuolar pH was raised in three ways: by addition of two weak bases (monensin and ammonium chloride) and by inhibition of the V-ATPase by bafilomycin (7). In all three cases, bacterial uptake and killing were greatly reduced (Fig. 3). Zero percent of amebae treated with bafilomycin, 3% of those treated with monensin, and 3% of those treated with ammonium chloride phagocytosed >10 bacteria/parasite. Similarly, 98% of amebae treated with bafilomycin, 48% of those treated with monensin, and 92% of those treated with ammonium chloride phagocytosed <6 bacteria. Bafilomycin also greatly inhibited uptake of RBC (Fig. 4). Three percent of bafilomycin-treated parasites phagocytosed >10 RBC per parasite, while 81% took up <6 RBC. These results, which are consistent with the coincidental selection of amebic lysis of host cells, are likely secondary to inhibition of amebic lysozyme and PFP, each of which has an acid pH optimum (23, 27, 28, 48). Inhibition of vacuolar acidification also blocks killing of bacteria by macrophages (18).

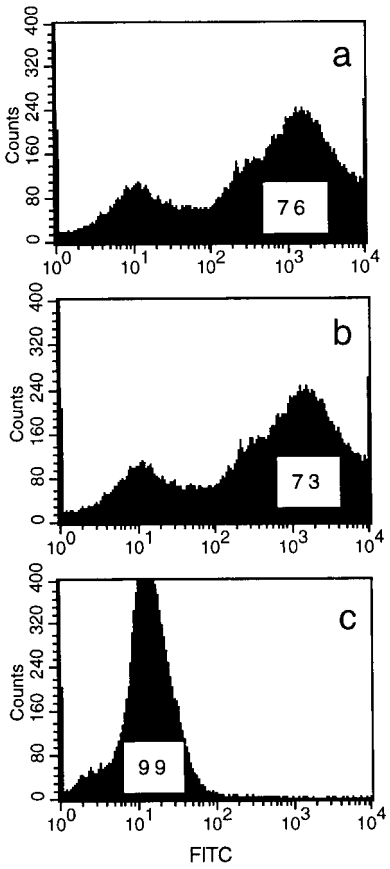

FIG. 6. FACS analyses of pinocytosis of FITC-dextran by nontransformed parasites plus or minus wortmannin and p21$^{racA\text{-}V12}$ transformants. About 76% of nontransformed amebae (a) and 73% of p21$^{racA\text{-}V12}$ transformants (b) showed extensive pinocytosis of FITC-dextran. In contrast, 100 nM wortmannin completely inhibited uptake of FITC-dextran (c).

Inhibition of amebic cysteine proteinase and other proteases had no effect on phagocytosis. Inhibition of amebic cysteine proteinase by E-64 blocks amebae from forming liver abscesses in vivo (51). In contrast, E-64 and three other cysteine proteinase inhibitors (*Z*-L-Leu-L-Tyr-CHN_2, phenylmethylsulfonyl fluoride, and leupeptin) had no effect on amebic phagocytosis of bacteria and RBC. These results suggest that the cysteine proteinase is not necessary for lysis of bacteria and RBC. Whether protease inhibitors block degradation of proteins released from lysed bacteria and RBC could not be determined.

DISCUSSION

Comparison of amebic phagocytosis with that of macrophages. Multiple methods developed to examine macrophage function were used for the first time to study amebic phagocytosis: (i) overexpression of p21$^{racA\text{-}V12}$, which lacks GTPase activity and so is fixed in the active state, (ii) incubation of parasites with fluorescent beads and GFP-labeled bacteria, and (iii) addition of wortmannin and bafilomycin to phagocytosing parasites (4, 7, 17, 22, 25, 37, 38, 45, 52, 54). Although amebae diverged from the main eukaryotic lineage about a billion years ago, there are numerous similarities between amebic killing of bacteria and that by human leukocytes. Like macrophages, amebae appear to need intact p21^{racA}, PI 3-kinase, and V-ATPase for phagocytosis of bacteria and RBC, and amebae may be activated to kill host epithelial cells by incubation with bacteria (4, 12, 18, 25, 37, 41). Like lymphocytes, amebae have

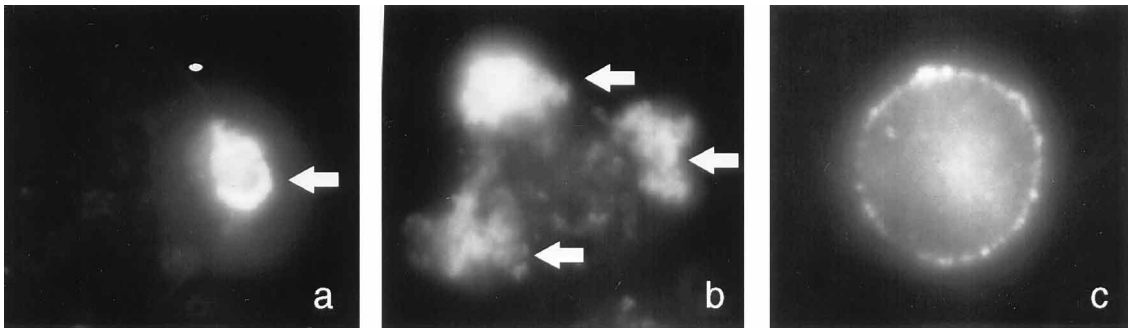

FIG. 7. Fluorescence microscopy of ConA capping by nontransformed amebae and p21$^{racA\text{-}V12}$ transformants. ConA accumulated into a single, tight cap on the surface of nearly 100% of nontransformed cells (a). In contrast, 19% of p21$^{racA\text{-}V12}$ transformants had multiple ConA cap sites on the same cell (b), while ConA was evenly distributed on the surface of 10% of p21$^{racA\text{-}V12}$ transformants (c).

PFP (homologous to NK lysin), which lyse bacteria and eukaryotic cells (3, 27, 28). Amebae also have lysozyme and other proteases capable of attacking the bacterial cell wall and of degrading bacterial proteins (9, 23, 24, 39, 51). Amebae differ from macrophages in that the parasite phagocytoses unopsonized bacteria and nonsenescent RBC, and killing is performed in the absence of oxygen and its reactive metabolites (25).

Overexpression of p21$^{racA\text{-}V12}$ in cultured amebae had numerous effects that might be expected: inhibition of capping and decreased phagocytosis of mucin-coated beads, RBC, and bacteria (2, 13, 18, 21). Overexpression of p21$^{racA\text{-}V12}$ also had some less predictable effects: decreased rates of cytokinesis and formation of actin cups in the absence of external stimuli (5, 20). Although these overexpression experiments cannot demonstrate the normal function of the amebic p21^{racA}, they suggest possible functions in which this or other amebic p21^{rac} proteins might be involved. These experiments also suggest functions in which p21^{rac} might not be involved (e.g., pinocytosis and fusion of phagosomes and lysosomes) (30, 48).

Coincidental selection. The idea of coincidental selection is important to the extent that it explains how amebic pathogenicity is maintained without obvious survival advantage to the parasite (19, 29, 38). Bacterial lysis and epithelial cell lysis have at least five common mechanisms: lectin binding and amebapore lysis (shown in references 3, 27, 28, 32, and 42) and involvement of p21^{racA}, PI 3-kinase, and V-ATPase (shown here). Remarkably, p21$^{racA\text{-}V12}$ overexpression and PI 3-kinase inhibition have similar effects on phagocytosis but opposite effects on pinocytosis and capping. Although the experiments with the cysteine proteinase inhibitors failed to support the idea of coincidental selection, it is not difficult to imagine other functions for the amebic cysteine proteinases besides bacterial killing (e.g., autodegradation of parasite proteins in lysosomes or degradation of cyst wall by excysting parasites) (26, 48). Other likely examples of coincidental selection for amebic pathogenesis include unique fermentation enzymes that make it possible for parasites to reproduce under anaerobic conditions in the colonic lumen and in tissue abscesses and ameboid motility that allows parasites to capture bacteria and penetrate into host tissues (2, 13, 44).

What is not explained by the idea of coincidental selection is the failure of *E. dispar* parasites, which also consume bacteria in the colonic lumen, to cause tissue disease and the inability of amebae to reproduce and form cysts in the colonic lumen of other mammalian hosts (15, 40, 43). Although there are quantitative and qualitative differences in lectins, PFP, and cysteine proteinases of *E. histolytica* and *E. dispar*, it is possible that amebic tissue invasion is determined by factors unrelated to bacterial killing (9, 24, 28, 32, 39). For example, genetic studies of *Salmonella* bacteria have shown that a handful of virulence genes are involved in host recognition and invasion, while the vast majority of bacterial virulence genes are involved in transcriptional control, nutrient biosynthesis, and peptide resistance (19). When methods for gene knock-out and transposon-mediated mutagenesis are developed for amebae, numerous new genes of the parasite involved in tissue invasion will likely be identified and the idea of coincidental selection may be tested further.

ACKNOWLEDGMENTS

This work was supported in part by Public Health Service grant AI-33492 from the National Institutes of Health.

We offer thanks to Marianne Wessling-Resnick, Lester Kobzik, and John Godleski, all of the Harvard School of Public Health, for advice and reagents.

REFERENCES

1. **Adams, A. E. M., D. I. Johnson, R. M. Longnecker, B. F. Sloat, and J. R. Pringle.** 1991. *CDC42* and *CDC43*, two additional genes involved in budding and establishment of cell polarity in the yeast *Saccharomyces cerevisiae*. J. Cell Biol. **111:**131–142.
2. **Ahrets, P., P. Gounon, P. Sansonetti, and N. Guillen.** 1995. Myosin II is involved in capping and uroid formation in the human pathogen *Entamoeba histolytica*. Infect. Immun. **63:**4358–4367.
3. **Andersson, M., H. Gunne, B. Agerberth, A. Boman, T. Bergman, R. Sillard, H. Jornvall, V. Mutt, B. Olsson, H. Wigzell, A. Dagerlind, H. G. Boman, and G. H. Gudmundsson.** 1995. NK-lysin, a novel effector peptide of cytotoxic T and NK-cells. Structure and cDNA cloning of the porcine form, induction by interleukin 2, antibacterial and antitumour activity. EMBO J. **14:**1615–1625.
4. **Araki, N., M. T. Johnson, and J. A. Swanson.** 1996. A role for phosphoinositide 3-kinase in the completion of macropinocytosis and phagocytosis by macrophages. J. Cell Biol. **135:**1249–1260.
5. **Bailey, G. B., D. B. Day, and G. W. Gasque.** 1985. Rapid polymerization of *Entamoeba histolytica* actin induced by interaction with target cells. J. Exp. Med. **162:**546–558.
6. **Biagi, F., and J. Portilla.** 1957. Comparison of methods of examining stools for parasites. Am. J. Trop. Med. Hyg. **6:**906–911.
7. **Bowman, E. J., A. Siebers, and K. Altendorf.** 1988. Bafilomycins: a class of inhibitors of membrane ATPases from microorganisms, animal cells, and plant cells. Proc. Natl. Acad. Sci. USA **85:**7972–7976.
8. **Brandt, H., and R. Perez Tamayo.** 1970. Pathology of human amebiasis. Hum. Pathol. **1:**351–385.
9. **Bruchhaus, I., T. Jacobs, M. Leippe, and E. Tannich.** 1996. Entamoeba histolytica and Entamoeba dispar: differences in numbers and expression of cysteine proteinase genes. Mol. Microbiol. **22:**255–263.
10. **Bush, J., K. Franek, and J. Cardelli.** 1993. Cloning and characterization of seven novel *Dictyostelium discoideum rac*-related genes belonging to the *rho* family of GTPases. Gene **136:**61–68.
11. **Chen, W., H. H. Lim, and I. Lim.** 1993. A new member of the *ras* superfamily, the *rac1* homologue from *Caenorhabditis elegans*. J. Biol. Chem. **268:**320–324.
12. **Deikmann, D., A. Abo, C. Johnston, A. W. Segal, and A. Hall.** 1994. Interaction of Rac with p67^{phox} and regulation of phagocytotic NADPH oxidase activity. Science **265:**531–537.

13. **de la Garza, M., B. Gallegos, and I. Meza.** 1989. Characterization of a cytochalasin D-resistant mutant of *Entamoeba histolytica*. J. Protozool. **36:** 556–560.
14. **Descoteaux, S., Y. Yi, and J. Samuelson.** 1994. Cloning of *Entamoeba* genes encoding proteolipids of putative vacuolar proton-translocating ATPases (V-ATPases). Infect. Immun. **62:**3572–3575.
15. **Diamond, L. S., and C. G. Clark.** 1993. A redescription of *Entamoeba histolytica* Schaudinn, 1903 (emended Walker, 1911) separating it from *Entamoeba dispar* Brumpt, 1925. J. Eukaryot. Microbiol. **40:**340–344.
16. **Espinosa-Cantellano, M., and A. Martinez-Palomo.** 1994. *Entamoeba histolytica*: mechanism of surface receptor capping. Exp. Parasitol. **79:**424–435.
17. **Ghosh, S. K., A. Lohia, A. Kumar, and J. Samuelson.** 1996. Overexpression of P-glycoprotein gene 1 by transfected *Entamoeba histolytica* confers emetine-resistance. Mol. Biochem. Parasitol. **82:**257–260.
18. **Grinstein, S., A. Nanda, G. Lukacs, and O. Rotstein.** 1992. V-ATPases in phagocytic cells. J. Exp. Biol. **172:**179–192.
19. **Groisman, E. A., and H. Ochman.** 1994. How to become a pathogen. Trends Microbiol. **2:**289–294.
20. **Guillen, N.** 1996. Role of signaling and cytoskeletal rearrangements in the pathogenesis of *Entamoeba histolytica*. Trends Microbiol. **4:**191–197.
21. **Guillen, N. and P. Sansonetti.** 1997. Rac G, a small GTPase, regulates capping of surface receptors in *Entamoeba histolytica*. Arch. Med. Res. **28:**S129–S131.
22. **Hall, A.** 1994. Small GTP-binding proteins and the regulation of the actin cytoskeleton. Annu. Rev. Cell Biol. **10:**31–54.
23. **Jacobs, T., and M. Leippe.** 1995. Purification and molecular cloning of a major antibacterial protein of the protozoan parasite *Entamoeba histolytica* with lysozyme-like properties. Eur. J. Biochem. **231:**831–838.
24. **Keene, W. H., M. E. Hidalgo, E. Orozco, and J. H. McKerrow.** 1990. *Entamoeba histolytica*: correlation of the cytopathic effects of virulent trophozoite with secretion of a cysteine proteinase. Exp. Parasitol. **71:**199–206.
25. **Kobzik, L.** 1995. Lung macrophage uptake of unopsonized environmental particulates. J. Immunol. **155:**367–376.
26. **Lee, D. H., and A. L. Goldberg.** 1996. Selective inhibitors of the proteasome-dependent and vacuolar pathways of protein degradation in *Saccharomyces cerevisiae*. J. Biol. Chem. **271:**27280–27284.
27. **Leippe, M.** 1994. Cytolytic and anti-bacterial activity of synthetic peptides derived from amoebapore, the pore-forming peptide of *Entamoeba histolytica*. Proc. Natl. Acad. Sci. USA **91:**2602–2606.
28. **Leippe, M.** 1997. Amoebapores. Parasitol. Today **13:**178–183.
29. **Levin, B. R., and C. Svanborg Eden.** 1990. Selection and evolution of virulence in bacteria: an ecumenical excursion and modest suggestion. Parasitology **100:**S103–S115.
30. **Lohden-Bendinger, U., and T. Bakker-Grunwald.** 1990. Evidence for a vacuolar-type proton ATPase in *Entamoeba histolytica*. Z. Naturforsch. **45c:**229–232.
31. **Lohia, A., and J. Samuelson.** 1996. Heterogeneity of *Entamoeba histolytica rac* genes encoding p21^{rac} homologues. Gene **173:**205–208.
32. **Mann, B. J., B. E. Torina, T. S. Vedvick, and W. R. Petri, Jr.** 1991. Sequence of a cysteine-rich galactose-specific lectin of *Entamoeba histolytica*. Proc. Natl. Acad. Sci. USA **88:**3248–3252.
33. **Marsh, K., M. English, J. Crawley, and N. Peshu.** 1996. The pathogenesis of cerebral malaria in African children. Ann. Trop. Med. Parasitol. **90:**395–402.
34. **Martinez-Palomo, A., and M. Martinez-Baez.** 1983. Selective primary health care: strategies for control of disease in the developing world. X. Amebiasis. Rev. Infect. Dis. **5:**1093–1102.
35. **May, R. M., and R. M. Anderson.** 1990. Parasite-host coevolution. Parasitology **100:**S89–S101.
36. **Mirelman, D.** 1987. Ameba-bacterium relationship in amebiasis. Microbiol. Rev. **51:**272–284.
37. **Ninomiya, N., K. Hazeki, Y. Fukui, T. Seya, T. Okada, O. Hazeki, and M. Ui.** 1994. Involvement of phosphotidylinositol 3-kinase in Fcg receptor signaling. J. Biol. Chem. **269:**22732–22737.
38. **Nobes, C. D., and A. Hall.** 1995. Rho, Rac, and Cdc42 GTPases regulate the assembly of multimolecular focal complexes associated with actin stress fibers, lamellipodia, and filopodia. Cell **81:**53–62.
39. **Que, X., and S. L. Reed.** 1997. Role of extracellular cysteine proteinases in pathogenesis of *Entamoeba histolytica* invasion. Parasitol. Today **13:**190–194.
40. **Ravdin, J. I.** 1995. Amebiasis. State-of-the-art clinical article. Clin. Infect. Dis. **20:**1453–1464.
41. **Ravdin, J. I., P. H. Schlesinger, C. F. Murphy, I. Y. Gluzman, and D. J. Krogstad.** 1986. Acid intracellular vesicles and cytolysis of mammalian target cells by *Entamoeba histolytica* trophozoites. J. Protozool. **33:**478–486.
42. **Ravdin, J. I., J. E. John, L. I. Johnston, D. J. Innes, and R. L. Guerrant.** 1985. Adherence of *Entamoeba histolytica* trophozoites to rat and human colonic mucosa. Infect. Immun. **48:**293–297.
43. **Read, A. F.** 1994. The evolution of virulence. Trends Microbiol. **2:**73–76.
44. **Reeves, R. E.** 1984. Metabolism of *Entamoeba histolytica* Schaudinn, 1903. Adv. Parasitol. **23:**105–142.
45. **Ridley, A. J., H. F. Paterson, C. L. Johnston, D. Diekmann, and A. Hall.** 1992. The small GTP-binding protein rac regulates growth factor-induced membrane ruffling. Cell **70:**401–410.
46. **Rodriguez, M. A., and E. Orozco.** 1986. Isolation and characterization of phagocytosis- and virulence-deficient mutants of *Entamoeba histolytica*. J. Infect. Dis. **154:**27–32.
47. **Samuelson, J., N. Azikiwe, and P.-S. Shen.** 1995. Proton- and calcium ion-transporting ATPases of *Entamoeba histolytica*. Parasitol. Today **11:**417–420.
48. **Schlesinger, P.** 1988. Lysosomes and *Entamoeba histolytica*, p. 297–313. *In* J. I. Ravdin (ed.), Amebiasis: human infection by *Entamoeba histolytica*. Churchill Livingstone, New York, N.Y.
49. **Shinjo, K., J. G. Koland, M. J. Hart, V. Narasimhan, D. I. Johnson, T. Evans, and R. A. Cerione.** 1990. Molecular cloning of the gene for the human placental GTP-binding protein G_p (G25K): identification of the GTP-binding protein as the human homologue of the yeast cell-division-cycle protein CDC42. Proc. Natl. Acad. Sci. USA **87:**9853–9857.
50. **Skolnik, E. Y., B. Margolis, M. Mohammadi, E. Lowenstein, R. Fischer, A. Drepps, A. Ullrich, and J. Schlessinger.** 1991. Cloning of the PI 3 kinase-associated p85 utilizing a novel method for expression/cloning of target proteins for receptor tyrosine kinases. Cell **65:**83–90.
51. **Stanley, S. L., Jr., T. Zhang, D. Rubin, and E. Li.** 1995. Role of the *Entamoeba histolytica* cysteine proteinase in amebic liver abscess formation in severe combined immunodeficiency mice. Infect. Immun. **63:**1587–1590.
52. **Valdivia, R. H., A. E. Hromockyj, D. Monack, L. Ramakrishnan, and S. Falkow.** 1996. Applications for green fluorescent protein (GFP) in the study of host-pathogen interactions. Gene **173:**47–52.
53. **Wilson, I. A., H. L. Niman, R. A. Houghten, A. R. Cherenson, M. L. Connoly, and R. A. Lerner.** 1984. The structure of an antigenic determinant in a protein. Cell **37:**767–778.
54. **Wymann, M. P., G. Bulgarelli-Leva, M. J. Zvelebil, L. Pirola, B. Vanhaesebroek, M. D. Waterfield, and G. Panayoutou.** 1996. Wortmannin inactivates phosphoinositide 3-kinase by covalent modification of Lys-802, a residue involved in the phosphate transfer reaction. Mol. Cell. Biol. **16:**1722–1733.
55. **Yi, Y., and J. Samuelson.** 1994. Primary structure of the *Entamoeba histolytica* gene (Ehvma1) encoding the catalytic peptide of a putative vacuolar membrane proton-transporting ATPase (V-ATPase). Mol. Biochem. Parasitol. **66:**16–169.

Editor: J. M. Mansfield